Chemical Science

EDGE ARTICLE

View Article Online
View Journal | View Issue

CrossMark click for updates

Cite this: *Chem. Sci.*, 2015, **6**, 3606

A prochelator peptide designed to use heterometallic cooperativity to enhance metal ion affinity†

Bruno Alies, Jacob D. Wiener and Katherine J. Franz*

Received 16th February 2015
Accepted 22nd April 2015

DOI: 10.1039/c5sc00602c

www.rsc.org/chemicalscience

A peptide has been designed so that its chelating affinity for one type of metal ion regulates its affinity for a second, different type of metal ion. The prochelator peptide (PCP), which is a fusion of motifs evocative of calcium loops and zinc fingers, forms a 1 : 2 Zn : peptide complex at pH 7.4 that increases its affinity for Zn^{2+} ~3-fold in the presence of Tb^{3+} (log β_2 from 13.8 to 14.3), while the 1 : 1 luminescent complex with Tb^{3+} is brighter, longer lived, and 20-fold tighter in the presence of Zn^{2+} (log K from 6.2 to 7.5). This unique example of cooperative, heterometallic allostery in a biologically compatible construct suggests the possibility of designing conditionally active metal-binding agents that could respond to dynamic changes in cellular metal status.

Introduction

The intersections of metal homeostasis pathways have important ramifications for cellular function and dysfunction.[1] Crosstalk among Na^+, K^+, and Ca^{2+} regulatory pathways, for example, orchestrates changes in the relative concentrations of these s-block ions that form the basis of neuronal activity. Recognition is now focusing increasingly on how Ca^{2+} fluxes associated with cell signaling may induce dynamic mobiliza-tion and redistribution of d-block ions like Zn^{2+} and Cu^+.[2–5] Reciprocally, dynamic changes of Zn^{2+} may impinge on Ca^{2+} homeostasis.[6,7] Tools to explore this crosstalk are needed to better understand the complexity of interconnected metal pathways and ultimately remedy dysfunctional aspects.

As part of our efforts to design conditionally active prochelators that change their metal chelating ability in response to specific stimuli,[8,9] we envisioned biologically compatible molecules that could increase their metal binding affinity for one metal in response to dynamic changes in the concentration of a second metal. This kind of allosteric regulation of metal chelation has precedent in biology. For example, the antibacterial properties of the mammalian immunodefense protein calprotectin are related to its ability to bind Mn^{2+} and Zn^{2+},[10] the affinity for which increases in the presence of Ca^{2+}.[11–13] Other members of the S100 family of calcium-binding proteins contain Zn^{2+} binding sites that positively influence Ca^{2+} binding,[14] while others show negative allostery, suggesting that Zn^{2+} in these cases might inhibit these proteins' responses to Ca^{2+} signals.[15–17] An interesting example of differential binding based on oxidation state is the bacterial metal resistance protein CopK, which displays cooperative binding of Cu^+ and Cu^{2+}.[18]

The concept of allosteric regulation in biology has inspired numerous efforts to develop artificial receptor systems, including ones where one or both of the effector and substrate species is a metal ion.[19–21] Many of these systems do not operate in water and are not compatible with biological applications. The field of *de novo* peptide and protein design offers elegant examples of bio-inspired cooperativity, for example an artificial metallohydrolase that uses a Hg^{2+} binding site to stabilize a catalytic Zn^{2+} site,[22] and the use of metal templating to mediate cooperative assembly along protein surfaces to generate sophisticated multi-subunit protein arrays.[23] Recently, a β-peptide bundle was shown to exhibit positive allosteric cooperativity in water for binding two Cd^{2+} ions at distinct sites.[24] In these cases, cooperative metal binding serves to stabilize the overall construct for structural or catalytic purposes. In contrast, the goal for metal-activated prochelators is to influence the environment around the construct by altering metal concentrations in a synergistic way.

Results and discussion

Here we present the first ProChelator Peptide (PCP) that contains distinct binding sites for two different metal ions that bind cooperatively, meaning that coordination of one increases the affinity for the other. We specifically wanted to incorporate synergistic zinc and calcium binding sites, and chose to use Tb^{3+} (Tb) as a surrogate for Ca^{2+} due to its similar coordination preferences and useful luminescence.[25] A starting point for our

Department of Chemistry, Duke University, Durham, North Carolina 27708, USA. E-mail: katherine.franz@duke.edu

† Electronic supplementary information (ESI) available: Experimental procedures and Fig. S1–S9 showing plots of lifetime, absorbance, titration, HPLC and mass spectra. See DOI: 10.1039/c5sc00602c

design was a lanthanide binding tag (LBT) developed by Imperiali *et al. via* iterative redesign of classic calcium-binding loops.[26–28] The crystal structure of the optimized Tb–LBT complex revealed that a hydrophobic patch generated by flanking tyrosine and leucine residues helps to stabilize the loop and improve the K_d for Tb from 8 μM for the original construct to 57 nM for the LBT shown in Fig. 1.[28] We hypothesized that replacing the flanking hydrophobic residues with histidines and cysteines could generate constructs that use Zn^{2+} (Zn) as a stabilizing factor *via* formation of a Cys_2His_2 motif reminiscent of classic zinc fingers. The sequences of the resulting PCP and several control peptides are shown in comparison to the template LBT in Fig. 1.

To investigate possible synergistic binding of Tb and Zn to PCP, the peptide was titrated with Tb in the absence and presence of Zn (Fig. 2). Both the intensity and the lifetime of Tb luminescence are sensitive to coordination environment. Aqueous Tb^{3+} is only weakly luminescent, but close proximity of a chromophore like tryptophan sensitizes intense Tb emission, which is also enhanced by displacement of inner-sphere H_2O molecules that quench Tb emission. In the absence of Zn, the sensitized Tb emission for PCP plateaus after 1 equivalent of Tb has been added, suggesting 1 : 1 Tb : PCP stoichiometry (Fig. 2). If Zn is present either at the beginning (Fig. 2a, red squares) or end of the Tb titration (Fig. 2b, red squares), the intensity increases 150%. This boost in Tb emission maximizes at 0.5 equivalent of Zn, suggesting a 1 : 2 Zn : PCP ratio. The luminescence lifetime also increases dramatically, gaining +1.1 ms in the presence of Zn (Table 1 and Fig. S1†). These combined results indicate that Zn has a clear effect on the coordination

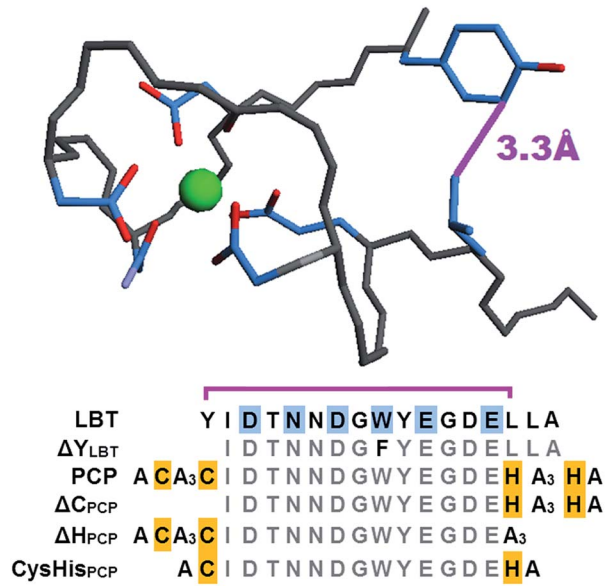

Fig. 1 Top: structure of the parent Tb–LBT complex (PDB 1TJB). For clarity, only the Tb-binding ligands and flanking Tyr_1 and Leu_{13} residues are shown, with their proximity emphasized by the purple line. Bottom: amino acid sequences of LBT, the ProChelator Peptide (PCP), and several controls. Putative Zn-binding residues are highlighted in yellow, with known Tb-binding residues of the LBT highlighted in cyan. Monodentate carboxylates from Asp1 and Asp5, bidentate carboxylates from Glu9 and Glu12, carboxamide O from Asn3, and backbone carbonyl O of Trp7 provide an 8-coordinate binding site for Tb^{3+}.

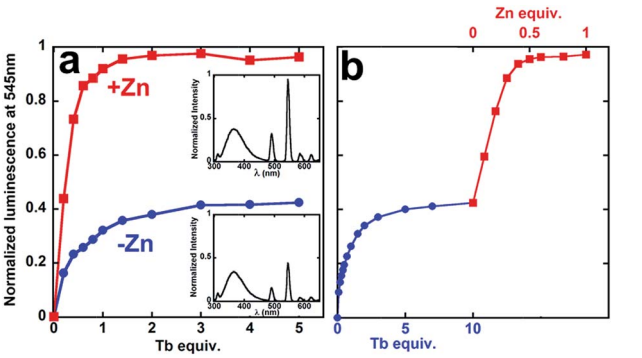

Fig. 2 Titrations of PCP with $TbCl_3$ monitored by sensitized Tb emission at 545 nm in the absence (blue, circles) or presence (red, squares) of $ZnSO_4$ that is either (a) present initially or (b) added subsequently to Tb. Insets show full emission spectra from 300–650 nm. Conditions: [PCP] = 0.5 μM; [Tb] = 0–5 μM; [Zn] = 0 or 0.5 μM; [HEPES] = 5 mM with 50 μM DTT, pH 7.4; λ_{ex} = 280 nm.

Table 1 Conditional association constants, pM values, and Tb luminescence lifetimes for peptides in the presence and/or absence of Zn^{2+} and/or Tb^{3+}. Conditions: 5 mM HEPES buffer pH 7.4 with 50 μM TCEP

	Zn association constant[a] ($\log \beta_2$) & pZn[b]		Tb association constant[c,d] ($\log K$) & pTb[b]		Lifetime (±0.1 ms)	
	(−) Tb	(+) Tb	(−) Zn	(+) Zn		
Peptides	$\log \beta_2$ (pZn)	$\log \beta_2$ (pZn)	$\log K$ (pTb)	$\log K$ (pTb)	(−) Zn	(+) Zn
LBT	≪10[e]	≪10[e]	7.8 ± 0.2[c] (8.3)	7.8 ± 0.2[c] (8.3)	2.5	2.5
ΔY_{LBT}	≪10[e]	≪10[e]	6.9 ± 0.1[d] (7.4)	6.8 ± 0.1[d] (7.3)	2.4	2.4
PCP	13.8 ± 0.2 (8.1)	14.3 ± 0.2 (8.6)	6.2 ± 0.2[d] (6.9)	7.5 ± 0.2[d] (8.1)	1.3	2.4
ΔC_{PCP}	10.6 ± 0.4 (6.3)	10.6 ± 0.4 (6.3)	5.5 ± 0.1[c] (6.5)	5.4 ± 0.1[c] (6.5)	1.0	1.0
ΔH_{PCP}	11.9 ± 0.2 (6.7)	11.9 ± 0.2 (6.7)	6.7 ± 0.1[c] (7.2)	6.4 ± 0.1[c] (7.0)	1.0	1.0
$CysHis_{PCP}$	11.5 ± 0.3 (6.5)	11.5 ± 0.3 (6.5)	6.2 ± 0.1[d] (6.9)	5.9 ± 0.1[d] (6.7)	1.2	1.5

[a] Zn affinity measured using PAR competition. [b] pM values calculated for [peptide] = 2 μM, [M1] = 0.5 μM and [M2] either zero or saturating. [c] Determined by direct titration. [d] Determined by competition with ΔY_{LBT} or LBT. [e] Does not compete with PAR. See ESI for further details.

environment of Tb. Furthermore, the observation that the order of metal addition does not impact the Zn-induced Tb emission indicates a system in dynamic equilibrium.

Formation of a 1 : 1 Tb : PCP complex was expected and consistent with previous studies using similar sequences.[26–28] While our original design imagined a 1 : 1 tetrahedral Zn binding site created by flanking Cys_2 and His_2 motifs of a single PCP, the data in Fig. 2 indicate a 1 : 2 Zn : PCP stoichiometry.

In order to test the importance of these flanking residues on Zn-dependent Tb luminescence, we synthesized control peptides that lack both N-terminal cysteines (ΔC_{PCP}), both C-terminal histidines (ΔH_{PCP}) or only have one Cys and one His on each end ($CysHis_{PCP}$). Substituting polar cysteines and histidines with alanines resulted in peptides with diminished solubility, whereas truncating the ends better replicated the solution properties of the parent peptide. The affinities for Zn and Tb were the same for truncated $CysHis_{PCP}$ compared to a longer Ala-substituted counterpart $A_4CysHis_{PCP}$ (ESI Fig. S3 and S5†), validating the truncation strategy. In contrast to PCP, Zn did not change the Tb luminescence lifetime of LBT, ΔC_{PCP}, or ΔH_{PCP}, and caused only a very minor 0.3 ± 0.1 ms increase in the case of $CysHis_{PCP}$. The three Cys and His truncated controls all showed a minor but consistent decrease in Tb emission intensity as a function of Zn, perhaps a result of direct competition with Tb for the carboxylate ligands in these cases. The control peptides have a lower affinity for Zn compared to PCP, in line with having fewer ligands available for Zn binding (Table 1). Even though the Tb binding site remains the same, Tb affinity varies slightly across this series, suggesting a contribution from the second coordination sphere, as seen for other metal–peptide complexes.[29] These combined observations from the control peptides support a model of Zn binding that requires at least one C-terminal histidine and one N-terminal cysteine from each peptide to form a 1 : 2 complex. This 1 : 2 stoichiometry and cysteine ligation are further supported by the appearance of a characteristic Zn–thiolate charge transfer at 230 nm that plateaus at 0.5 equiv. of added Zn (see Fig. S8†).[30,31] The absence of cooperative Zn and Tb binding by the control peptides highlights the uniqueness of the amino acid arrangement in PCP that fosters Zn-dependent changes in the Tb coordination, likely a consequence of a peptide conformational change.

To further investigate this structural change, we estimated the number of coordinated water molecules (q) on Tb by measuring the Tb lifetime at different ratios of H_2O/D_2O (Fig. 3 and S4†).[32] For Tb–PCP, a q value of 1.5 decreases to 0.5 when Zn is present, a reduction that is illustrated by a smaller variation of luminescence decay rate in the presence of Zn than in its absence (Fig. 3 red *vs.* blue, respectively). These data indicate that Zn binding to the PCP–Tb complex induces a conformational change that better shields Tb from water and even occludes an H_2O ligand from the inner coordination sphere. Concurrent with the increase in lifetime is an increase in emission intensity upon Zn binding (see Fig. S1† PCP), which suggests that the conformational change triggered by Zn more

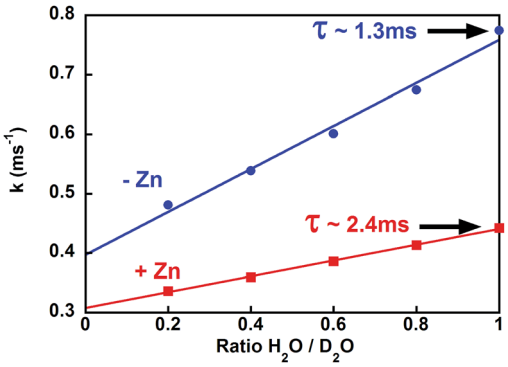

Fig. 3 Luminescence decay rates for PCP–Tb in the presence (red squares) or absence (blue circles) of Zn at several H_2O/D_2O ratios. Solid lines are the linear fit. Conditions: [PCP] = 2 μM; [Tb] = 5 μM; [Zn] = 0 or 2 μM; [HEPES] = 5 mM pH 7.4; [TCEP] = 50 μM.

favourably aligns the Trp for energy transfer to Tb, perhaps by improving the peptide's Tb affinity.

Measuring the binding affinity of PCP for Tb required a competitive ligand with specificity for Tb^{3+} over Zn^{2+}. Because the template LBT itself has negligible affinity for Zn (Table 1), we made a derivative, ΔY_{LBT}, that lacks the first tyrosine and replaces the tryptophan with phenylalanine. Deletion of Tyr_1 lowers Tb affinity,[28] and replacement of the Trp quiets the Tb emission (a remaining Tyr retains some luminescence). Fig. 4 displays a Tb competition experiment between PCP and ΔY_{LBT}. In the absence of Zn (Fig. 4, blue circles), the concentration of ΔY_{LBT} needed to displace half of the Tb from PCP is about 10 μM, whereas in the presence of Zn it is 50 μM. The conditional association constants of PCP for Tb are obtained from fitting these titration curves (Table 1). Expressed as dissociation constants, the K_d for Tb drops from 630 nM to 30 nM upon addition of Zn. Overall, this ~20-fold amplification in Tb affinity as a result of Zn is of the same magnitude as the effect of Ca on Zn or Mn binding to calprotectin,[11,12] a protein with over 200 amino acids and multiple Ca-binding sites.[13,33]

In order to explore the full cooperativity between Tb and Zn, we measured the affinity of PCP binding to Zn as a function of Tb by using the metal chelator 4-(2-pyridylazo)resorcinol (PAR),

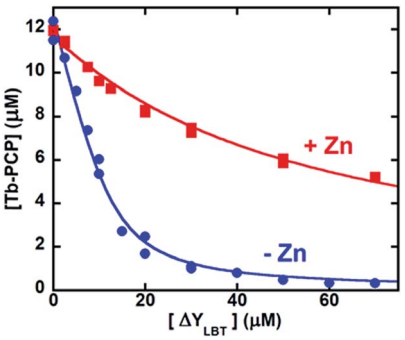

Fig. 4 Tb competition between PCP and ΔY_{LBT} in the presence (red squares) or absence of Zn (blue circles); solid lines represent the best fit. Conditions: [PCP] = 15 μM; [Tb] = 12 μM; [Zn] = 0 or 15 μM; [HEPES] = 5 mM pH 7.4; [TCEP] = 100 μM.

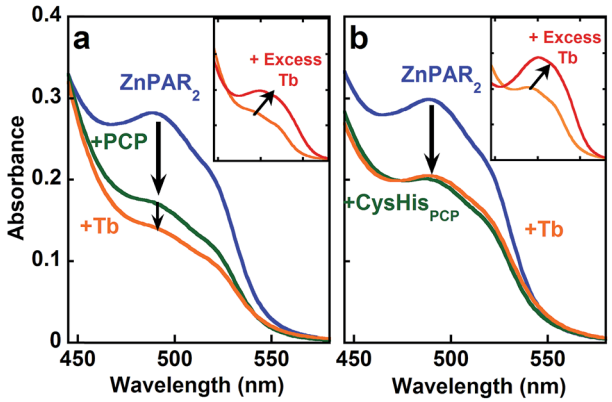

Fig. 5 UV-vis spectra of $Zn(PAR)_2$ (blue trace) followed by addition of PCP (a) or $CysHis_{PCP}$ (b) (long arrow to green trace), followed by addition of Tb (orange trace). Inset shows excess Tb (orange to red) produces a Tb–PAR complex. Conditions: [PAR] = 20 μM; [Zn] = 3 μM; [PCP] = 0–5 μM; [Tb] = 0–50 μM; [$CysHis_{PCP}$] = 0–30 μM; [HEPES] = 5 mM pH 7.4; [TCEP] = 100 μM.

which forms colored complexes with various metal ions. The $Zn(PAR)_2$ complex exhibits a band with a λ_{max} at 490 nm (Fig. 5a, solid blue line). The addition of PCP (solid green line) causes a decrease in intensity at 490 nm, suggesting removal of Zn from $ZnPAR_2$. Subsequent addition of Tb (solid orange line) leads to a further decrease at 490 nm, which suggests that the binding of Tb to PCP increases its affinity for Zn. This behavior is unique for PCP and is not observed for $CysHis_{PCP}$ (Fig. 5b) or other control peptides (Fig. S5†). If an excess of Tb is added (Fig. 5 inset, solid red line), another colored complex grows in with λ_{max} of 510 nm, which is consistent with formation of a Tb–PAR complex. Because the Zn and Tb–PAR complexes absorb at different wavelengths, the concentrations of the various species in solution can be calculated and the conditional affinity of PCP for Zn determined in the presence and absence of Tb (Table 1). A 3-fold increase in PCP's Zn affinity occurs in the presence of Tb, whereas the Zn affinity of the control peptides is unchanged. Although modest, this change in affinity is significant since metal concentrations in living system are regulated within a narrow range.

Combined, the data presented here show that PCP has the ability to bind both Tb and Zn in a cooperative manner. Direct comparison of PCP Tb and Zn affinity constants (Table 1) is misleading because of their differing stoichiometries (1 : 1 *vs.* 1 : 2), therefore we calculated pM values (−log[M]free) to assess how much free (uncomplexed) metal would be present under a defined set of conditions. The pM values in Table 1 were calculated for 0.5 μM M_1 and 2 μM apo-peptide or M_2-loaded peptide, with a wider range of M_1 concentrations shown in Fig. 6. For PCP, a pZn of 8.1 increases to 8.6 in the presence of Tb, while its pTb goes from 6.9 to 8.1 for the apo and Zn-loaded forms, respectively. In many cases, allostery is only observable for the stronger binding substrate in the presence of a weaker binding effector,[20] but in this case the similarity in Zn and Tb affinities enables observation of the influence of metal binding in both directions, meaning Zn and Tb are both substrate and effector for each other.

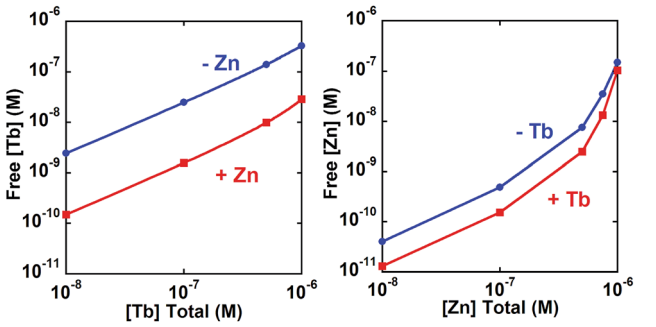

Fig. 6 Calculated concentration (logarithmic scale) of unbound Tb (left panel) or Zn (right panel) in the presence or absence of the second metal. Free metal calculated at 2 μM PCP.

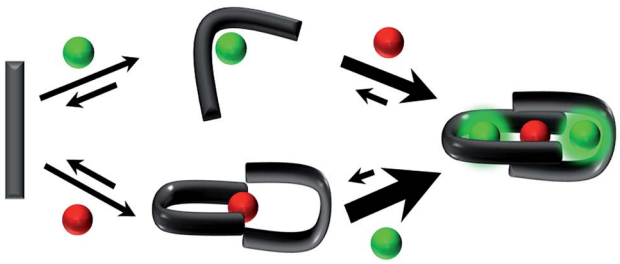

Scheme 1 Proposed model of cooperative metal binding of two different metal ions (Tb^{3+} green, Zn^{2+} red) to prochelator peptide PCP (flexible black cylinder). The higher Tb emission observed in the presence of Zn is emphasized by a glow around Tb.

Conclusions

The present work establishes that a simple peptide built from native amino acids and designed to harbor two metal binding sites can self assemble into a heterometallic species in which the chelation of one metal ion enhances the affinity for another, and *vice versa* (Scheme 1). This concept has been exemplified with Tb^{3+} and Zn^{2+} as the allosteric partners, but the readily accessible peptide template could be reconfigured for targeting other metals. Such constructs may be interesting for studying heterometallic allostery in aqueous environments, and potentially for controlling free metal ion concentrations in complex environments like cells and organisms, where dynamic alterations in various metal concentrations influence function.

Acknowledgements

We thank the NSF (CHE-1152054) and Duke University for financial support, and Alex Owens for early data collection.

Notes and references

1 D. S. Folk, F. Kielar and K. J. Franz, in *Comprehensive Inorganic Chemistry II*, ed. J. Reedijk and K. Poeppelmeier, Elsevier, Amsterdam, 2013, pp. 207–240.
2 W. Maret, *Proc. Natl. Acad. Sci. U. S. A.*, 2001, **98**, 12325–12327.

3 Y. Qin, P. J. Dittmer, J. G. Park, K. B. Jansen and A. E. Palmer, *Proc. Natl. Acad. Sci. U. S. A.*, 2011, **108**, 7351–7356.
4 S. C. Dodani, D. W. Domaille, C. I. Nam, E. W. Miller, L. A. Finney, S. Vogt and C. J. Chang, *Proc. Natl. Acad. Sci. U. S. A.*, 2011, **108**, 5980–5985.
5 A. Grubman, S. A. James, J. James, C. Duncan, I. Volitakis, J. L. Hickey, P. J. Crouch, P. S. Donnelly, K. M. Kanninen, J. R. Liddell, S. L. Cotman, M. D. de Jonge and A. R. White, *Chem. Sci.*, 2014, **5**, 2503–2516.
6 J. Liu, J. E. Kohler, A. L. Blass, J. A. Moncaster, A. Mocofanescu, M. A. Marcus, E. A. Blakely, K. A. Bjornstad, C. Amarasiriwardena, N. Casey, L. E. Goldstein and D. I. Soybel, *PLoS One*, 2011, **6**, e19638.
7 D. Guo, Y. Du, Q. Wu, W. Jiang and H. Bi, *Arch. Biochem. Biophys.*, 2014, **560**, 44–51.
8 L. K. Charkoudian, D. M. Pham and K. J. Franz, *J. Am. Chem. Soc.*, 2006, **128**, 12424–12425.
9 D. S. Folk and K. J. Franz, *J. Am. Chem. Soc.*, 2010, **132**, 4994–4995.
10 S. M. Damo, T. E. Kehl-Fie, N. Sugitani, M. E. Holt, S. Rathi, W. J. Murphy, Y. Zhang, C. Betz, L. Hench, G. Fritz, E. P. Skaar and W. J. Chazin, *Proc. Natl. Acad. Sci. USA*, 2013, **110**, 3841–3846.
11 J. A. Hayden, M. B. Brophy, L. S. Cunden and E. M. Nolan, *J. Am. Chem. Soc.*, 2013, **135**, 775–787.
12 M. B. Brophy, J. A. Hayden and E. M. Nolan, *J. Am. Chem. Soc.*, 2012, **134**, 18089–18100.
13 D. M. Gagnon, M. B. Brophy, S. E. J. Bowman, T. A. Stich, C. L. Drennan, R. D. Britt and E. M. Nolan, *J. Am. Chem. Soc.*, 2015, **137**, 3004–3016.
14 J. Baudier, N. Glasser and D. Gerard, *J. Biol. Chem.*, 1986, **261**, 8192–8203.
15 M. Koch, S. Bhattacharya, T. Kehl, M. Gimona, M. Vašák, W. Chazin, C. W. Heizmann, P. M. H. Kroneck and G. Fritz, *Biochim. Biophys. Acta*, 2007, **1773**, 457–470.
16 M. C. Bauer, H. Nilsson, E. Thulin, B. Frohm, J. Malm and S. Linse, *Protein Sci.*, 2008, **17**, 760–767.
17 H. M. Botelho, M. Koch, G. Fritz and C. M. Gomes, *FEBS J.*, 2009, **276**, 1776–1786.
18 L. X. Chong, M.-R. Ash, M. J. Maher, M. G. Hinds, Z. Xiao and A. G. Wedd, *J. Am. Chem. Soc.*, 2009, **131**, 3549–3564.
19 M. Elhabiri and A.-M. Albrecht-Gary, *Coord. Chem. Rev.*, 2008, **252**, 1079–1092.
20 C. Kremer and A. Lützen, *Chem.–Eur. J.*, 2013, **19**, 6162–6196.
21 L. Kovbasyuk and R. Krämer, *Chem. Rev.*, 2004, **104**, 3161–3188.
22 M. L. Zastrow, A. F. A. Peacock, J. A. Stuckey and V. L. Pecoraro, *Nat. Chem.*, 2011, **4**, 118–123.
23 J. D. Brodin, X. I. Ambroggio, C. Tang, K. N. Parent, T. S. Baker and F. A. Tezcan, *Nat. Chem.*, 2012, **4**, 375–382.
24 J. P. Miller, M. S. Melicher and A. Schepartz, *J. Am. Chem. Soc.*, 2014, **136**, 14726–14729.
25 J.-C. G. Bunzli and C. Piguet, *Chem. Soc. Rev.*, 2005, **34**, 1048–1077.
26 M. Nitz, K. J. Franz, R. L. Maglathlin and B. Imperiali, *ChemBioChem*, 2003, **4**, 272–276.
27 K. J. Franz, M. Nitz and B. Imperiali, *ChemBioChem*, 2003, **4**, 265–271.
28 M. Nitz, M. Sherawat, K. J. Franz, E. Peisach, K. N. Allen and B. Imperiali, *Angew. Chem., Int. Ed.*, 2004, **43**, 3682–3685.
29 B. Alies, C. Bijani, S. Sayen, E. Guillon, P. Faller and C. Hureau, *Inorg. Chem.*, 2012, **51**, 12988–13000.
30 M. Vasak and J. H. R. Kagi, *Met. Ions Biol. Syst.*, 1983, **15**, 213–273.
31 L.-J. Jiang, M. Vašák, B. L. Vallee and W. Maret, *Proc. Natl. Acad. Sci. U. S. A.*, 2000, **97**, 2503–2508.
32 W. D. Horrocks and D. R. Sudnick, *J. Am. Chem. Soc.*, 1979, **101**, 334–340.
33 I. P. Korndörfer, F. Brueckner and A. Skerra, *J. Mol. Biol.*, 2007, **370**, 887–898.